



An intelligent Approach to Combinational Load Shedding with Tracing

Reactive Power based on Genetic Algorithm

Ghazanfar SHAHGHOIAN*, Bahman ZAHEDI

Department of Electrical Engineering, Najafabad Branch, Islamic Azad University Najafabad, Isfahan, Iran

Received: 24.07.2016; Accepted: 18.11.2016

Abstract. Stability of both voltage and frequency in power systems is the basis of the electricity generation. Load shedding is one the last strategies to stabilize a power system. However, the conventional load shedding schemes do not consider the reactive power as a direct participation in load shedding, which is essential for the voltage stability. To fill this gap, we propose a new combinational under frequency load shedding (UFLS) and Under Voltage Load Shedding (UVLS), considering reactive and active power simultaneously, and using non-dominated sorting genetic algorithm (NSGA II) in this paper. The location of bus loads, the reactive power and the active power consumption at each bus are used as GA control variables. This method is tested on the modified IEEE 39-bus system. The results of simulations validate the proficiency of proposed method in stabilizing the frequency and voltage of the power system.

Keywords: Power system stability, Genetic algorithms, frequency load shedding, voltage load shedding

Genetik Algoritma Tabanlı İzleme Reaktif Güçlü Bileşimli Yük Atması için Akıllı bir Yaklaşım

Özet. Güç sistemlerinde gerilim ve frekansın dengesi elektrik üretiminin temelini oluşturur. Yük atma, bir güç sistemini stabilize etmek için son stratejilerden biridir. Bununla birlikte, geleneksel yük atma planları, reaktif gücün, gerilim kararlılığı için, gerekli olan yük dökülmesine doğrudan katılım olarak düşünmemektedir. Bu boşluğu doldurmak için, aynı anda reaktif ve aktif güç dikkate alınarak ve frekans yük atma (UFLS) ve Düşük Voltaj Yük Atma (UVLS) altında yeni bir kombinasyonel yöntem önerilmiş ve bu makalede dominant olmayan sıralama genetik algoritması (NSGA II) kullanılmıştır. Veri yolu yüklerinin konumu, reaktif güç ve her veri yolundaki aktif güç tüketimi GA kontrol değişkenleri olarak kullanılır. Bu yöntem, değiştirilmiş IEEE 39-veri yolu sisteminde test edilmiştir. Simülasyonların sonuçları, güç sisteminin frekansını ve voltajını dengelemek için önerilen yöntemin yeterliliğini doğrulamaktadır.

Anahtar kelimeler: Güç sistemi kararlılığı, Genetik algoritmalar, frekans yük atması, voltaj yükü atması

1. INTRODUCTION

Increasing of large disturbances has resulted in incremental utilization of under frequency load shedding (UFLS) and under voltage load shedding (UVLS) in comparison with the past [1,2]. Usually, these two schemes work independently from each other, and are not designed in an integrated way to exploit their combined effect on load shedding [3]. Combinational load shedding schemes cope with large disturbances more effectively, as they use more controlling parameters of power systems [4,5].

The best method of load shedding in a power system is a technique to shed fewer burdens in a shorter time to retain the transient constancy of the power system. This is what that the conventional load shedding schemes are incapable of dealing with, for the reason that they are too dilatory and also they may shed loads more than sufficient amount [6] and [7]. Intelligent networks are employed to recognize the best shedding approach to optimize the time taking and the amount of load shedding. Genetic algorithm (GA) is one of the intelligent analytical methods that has been employed extensively in load shedding [8,9]. Since the performance of the GA is based on the maximum/minimum amount of adaptation of data to an objective function; it could play an effective role to reduce the number of load

* Corresponding author. *Email address:* shahgholian@iaun.ac.ir

buses disconnection in a power system. In [10] GA is employed to minimize the shed load using under frequency relays so that the shed load at the first stage is the largest amount and the shed loads at the subsequent stages decrease gradually. In [11], utilizes GA to optimize load shedding and decide how to restore power supply after its outage. In [12], GA is exploited to optimize the coordinated voltage control in combinational hard conditions that tested on IEEE 39-bus test system. In [13], applies GA to control load frequency owing the fact that it could be designed for non-linear parameters controlling in a power system. However, reactive power information is employed rarely in load shedding plans, unexpectedly in current intelligent and combinational schemes that leads to deficiency of load shedding strategies.

Reactive power tracing effect on determination of the power system stability along with assessment of other parameters, suitable buses recognition, and minimum reactive and active power to be shed is utilized in this paper to reduce the time and the amount of load shedding. The modified IEEE 39-Bus system is employed to assess the proposed load shedding scheme. The results corroborate an optimal efficient load shedding method. The structure of this paper is organized as follows: necessity of utilization of a combinational load shedding is described in Section II. The determination method of Load shedding distribution is introduced in Section III, while Section IV represents a Genetic Algorithm employed in this paper. Section V gives a summarized description of load shedding distribution schemes compared in this paper. Test system for the assessment of the proposed load shedding method is introduced in Section VI, and Section VII depicts simulated results. Section VIII summarizes the conclusions.

2. COMBINATIONAL LOAD SHEDDING

Traditional load shedding methods do not have the potential to deal with combined instabilities, as discussed in [14] and [15]. Therefore combinational load shedding schemes are alternatively being used [16] and [17]. Nevertheless, the existing methods for combinational load shedding still exclude controlled reactive power from the direct participation in load shedding that results in an inefficient load shedding [18]. Since the proposed load shedding scheme in this paper is based on simultaneous voltage (reactive power) and frequency (active power) data analysis, the utilization of global triggers is recommended. For this reason we consider λ_{min}, f_c and df/dt as the trigger with corresponding thresholds:

- λ_{min} : the minimum eigenvalue of the Jacobian matrix smaller than zero; the bus voltage magnitude limits are (0.95 pu, 1.05 pu) for the generator buses, whereas (0.9 pu, 1.1 pu) for the rest of the buses [19].
- f_c : out of the normal frequency range (59.5, 60.5) Hz;
- df/dt : the rate of change of frequency in the abnormal range of (-1.5, -0.2) Hz/s.

The rate of change of frequency is calculated as in Eq. (1) and Eq. (2) as described in [16]:

$$\Delta P = \frac{2 \sum_{i=1}^N H_i \cdot S_i}{f_n} \cdot \frac{df_c}{dt} = \xi \frac{df_c}{dt} \quad (1)$$

$$\frac{df_c}{dt} = \frac{\sum_{i=1}^N H_i \cdot S_i \cdot \frac{df_{Gi}}{dt}}{\sum_{i=1}^N H_i \cdot S_i} \quad (2)$$

where ΔP is total active power imbalance (pu.), H_i is inertia constant of the i th generator; S_i is rated apparent power of the i th generator; f_n is rated system frequency (60 Hz); f_{Gi} is frequency of the i th generator; f_c is frequency for the equivalent inertia center; N is the total number of generators. ξ is a constant value:

$$\xi = \frac{2}{f_n} \sum_{i=1}^N H_i \cdot S_i \quad (3)$$

3. IMPROVED POWER IMBALANCE ESTIMATION

In the classic system frequency response (SFR) model, only inertia constant of generator and frequency information is considered [20, 21]. However, as discussed in [7] and suggested in [22], the load model with voltage and frequency dependence should also be included in the design for UFLS in order to achieve accurate active power imbalance estimation. Since the voltage variation is always much faster and larger than the change of frequency [16] and [7], only the voltage dependence of the load model as it is explained in (3), is applied to the load shedding scheme in [16] and [7]. Based on this load model, the method proposed in [7] is adopted in this paper to improve both active power and reactive power imbalance estimation. This amount of active power and reactive power can be employed as fundamental loads that should be shed after each scenario.

$$S_{Lj} = \sqrt{(P_{Lj})^2 + (Q_{Lj})^2} = \sqrt{\left(P_{L0,j} \times \left(\frac{V_j}{V_{0,j}}\right)^{\alpha_j}\right)^2 + \left(Q_{L0,j} \times \left(\frac{V_j}{V_{0,j}}\right)^{\beta_j}\right)^2} \quad (4)$$

where S_{Lj} is rated apparent power of the j th load bus; P_{Lj} and Q_{Lj} are the current active and reactive power load of the j th load bus, respectively; $P_{L0,j}$ and $Q_{L0,j}$ are the initial active and reactive power load of the j th load bus before the disturbance, respectively; P_L and Q_L are the current total active and reactive power load of all the buses, respectively; V_j is the current voltage magnitude of the j th load bus after the disturbance; $V_{0,j}$ is the initial voltage magnitude of the j th load bus before the disturbance; α_j and β_j are factors that depict the active and reactive power dependence of the load on voltage deviations, which are set to 1 and 2, respectively, as introduced in [6]; M is total number of load buses. It is necessary to stress that in reality, the factors α_j and β_j are usually not zero and vary not only from one part of the system to another but also from time to time. As mentioned in [16], the total active power imbalance of all the generators considering the voltage dependent load modeling is defined as

$$\Delta P_{deficit} = \Delta P + \sum_{j=1}^M P_{L0,j} \times \left[\left(\frac{V_j}{V_{0,j}}\right)^{\alpha_j} - 1 \right] \quad (5)$$

where ΔP is the total active power imbalance of all the generators based on the classic SFR model, neglecting the voltage dependence and frequency. Under the assumption that the power factor between the total active power deficit $\Delta P_{deficit}$ and reactive power deficit $\Delta Q_{deficit}$ is identical to the one between total active power load P_{L0} and reactive power load Q_{L0} before load shedding, once $\Delta P_{deficit}$ is estimated by Eq. (4), it is proposed to calculate $\Delta Q_{deficit}$ as follows:

$$\Delta Q_{deficit} = \frac{Q_{L0}}{P_{L0}} \cdot \Delta P_{deficit} \quad (6)$$

V-Q sensitivity at bus j can be computed by:

$$VQS_j = \frac{\partial V_j}{\partial Q_j} \quad (7)$$

where V_j and Q_j are voltage and reactive power at bus j , respectively. A positive value of the VQS_j presents that the relationship between the change of voltage and the change of reactive power is stable at the bus and the voltage is more sensitive to reactive power variation as increases. A negative value of VQS_j represents an unstable operating condition.

To consider active and reactive power information jointly in the determination load shedding distribution strategy, two indices, the load shedding distribution factor for active power (LSDFP) and load shedding distribution factor for reactive power (LSDFQ) for the load buses, are defined. LSDFP and LSDFQ can be obtained by Eq. (7), which is proportional to the total active and reactive power imbalance, respectively, as indicated in Eq. (8). As observed in Eq. (7), information about frequency and active power are included in LSDFP, while voltage and reactive power information are calculated together for LSDFQ [16].

$$\left\{ \begin{array}{l} LSDFP_j = \frac{\Delta f_{Lj} \cdot P_j}{\sum_{j=1}^M (\Delta f_{Lj} \cdot P_j)} \\ LSDFQ_j = \frac{VQS_j \cdot Q_j}{\sum_{j=1}^M (VQS_j \cdot Q_j)} \end{array} \right. \quad (8)$$

$$\left\{ \begin{array}{l} \Delta P_{Lj} = \Delta P_{deficit} \cdot LSDFP_j \\ \Delta Q_{Lj} = \Delta Q_{deficit} \cdot LSDFQ_j \end{array} \right. \quad (9)$$

where Δf_{Lj} is frequency deviation to the rated frequency (60 Hz in this paper) of the j th load bus.

4. SECOND EDITION OF MULTI OBJECTIVE GENETIC ALGORITHM

The second edition of Non-Dominated Sorting Genetic Algorithm (NSGA-II) is a multi-objective GA that is employed for load shedding adoption and identification of the weakest load buses of the test power system, in case of disturbances, which is using a set of solutions (Pareto Front), instead of a single one. A main objective function and a sub-function are determined to optimize the load shedding scheme using NSGA-II. The main objective function is considered as in Eq. (9), and the sub-function is defined by the equation Eq. (10), as described in [10]:

$$F_{main} = \sum_{i=1}^N \sqrt{P_{G0,i}^2 + Q_{G0,i}^2} - \sum_{i=1}^N \sqrt{(P_{Gi}^c)^2 + (Q_{Gi}^c)^2} \quad (10)$$

$$F_{aux} = \beta^* \cdot \sum_{j=1}^M \alpha_j^* ([P_{L0,j} - P_{Lj}^c] + [Q_{L0,j} - Q_{Lj}^c]) \quad (11)$$

where G , L and C are generator, load and contingency indices, respectively; $P_{G0,i}$ and $Q_{G0,i}$ are the pre-disturbance active and reactive power generation of the i th bus; P_{Gi}^c and Q_{Gi}^c are the current active and reactive power generation of the i th bus, related to the c th contingency; P_{Lj}^c and Q_{Lj}^c are the current active and reactive power load of the j th load bus, related to the c th contingency; β^* is a constant parameter to make F_{aux} as close as possible to F_{main} ; α^* is the importance index computed so that the greatest amount of load shedding belongs to the weakest load buses. According to Eq. (3) the weakest load buses are the ones that are highly affected by a specific disturbance. (i.e. there is the most difference between the current voltage magnitude of the j th load bus after the disturbance and the initial voltage

magnitude of the j th load bus before the disturbance). α_j^* is defined as Eq. (11); where γ is the difference between the absolute value of the current voltage magnitude of the j th load bus after a disturbance to the initial voltage magnitude of the j th load bus before the disturbance and number 1.

$$\alpha_j^* = \begin{cases} 1 & , \quad 0 \leq \gamma < 0.2 \\ 3 & , \quad 0.2 \leq \gamma < 0.5 \\ 6 & , \quad 0.5 \leq \gamma < 0.8 \\ 8 & , \quad 0.8 \leq \gamma \leq 1 \end{cases} \quad (12)$$

The selected weakest load buses for the first stage of load shedding and the amount of both active power and reactive power that must be shed from these load buses are defined as GA controlled variables. A summary of NSGA-II performance to recognize the weakest load buses and the amount of active power and reactive power of the j th load bus that must be shed from the selected weakest load buses is described in Fig. 1.

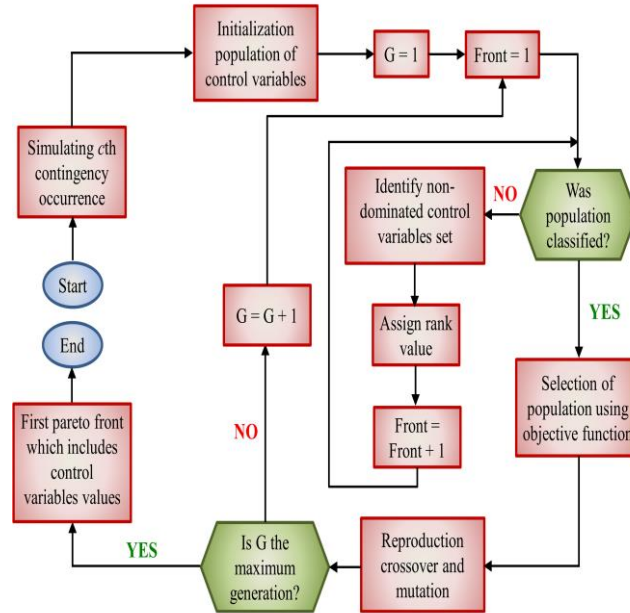


Fig. 1. Basic steps of the NSGA-II employed to minimize the combinational load shedding problem [13].

5. CLASSIFICATION OF LOAD SHEDDING METHODS

Conventional load shedding distribution schemes do not consider reactive power information in the load shedding directly. In this paper, we compare the load shedding distribution method using power flow tracing to identify the active and reactive power imbalance denotes (M1), which it was introduced in [16] as the best load shedding method, and the proposed load shedding distribution method using GA to identify the weakest buses denotes (M2). These two methods in addition to all the necessary information for each load shedding distribution method are summarized in Table I. M1: corresponds to distribution method as defined in Eq. (7) and Eq. (8), proposed in [16]; M2: corresponds to the distribution method as mainly defined in Eq. (9)–(11), proposed in this paper.

An intelligent Approach to Combinational

Table I. Classification of methods for load shedding.

L.S. method No.	Factors in load shedding distribution	
	LSDFP	LSDFQ
M1	Active power of j^{th} bus (computed by power flow), j^{th} bus frequency deviation	Reactive power of j^{th} bus (computed by power flow), j^{th} bus frequency deviation
M2	Active power of j^{th} bus according to $(V_j/V_{o,j})^{\alpha_j}$ (computed by GA), j^{th} bus frequency deviation	Reactive power of j^{th} bus according to $(V_j/V_{o,j})^{\alpha_j}$ (computed by GA), j^{th} bus frequency deviation

6. SIMULATION RESULTS

As a typical transmission network with multiple generators and loads, IEEE 39-Bus test system (New England network) is selected for the test system in this paper. According to [16], seen from Fig. 2, a small modification is applied to divide bus 39 into bus 39 with a load and bus 40 located with a generator, which are connected by a transmission line with low impedance, while the small load in bus 31 is neglected. A short summary of the network characteristics is represented in Table II. According to [19] the nominal generation of the active power and reactive power is 7066.65 MW and 1694.22 MVar, respectively, while the maximum active power and reactive power output are 8625 MW and 5345.3 MVar respectively; nominal active power consumption is 7011.66 MW and nominal reactive power consumption is 1620.22 MVar. The base power of the test system is 100 MVA.

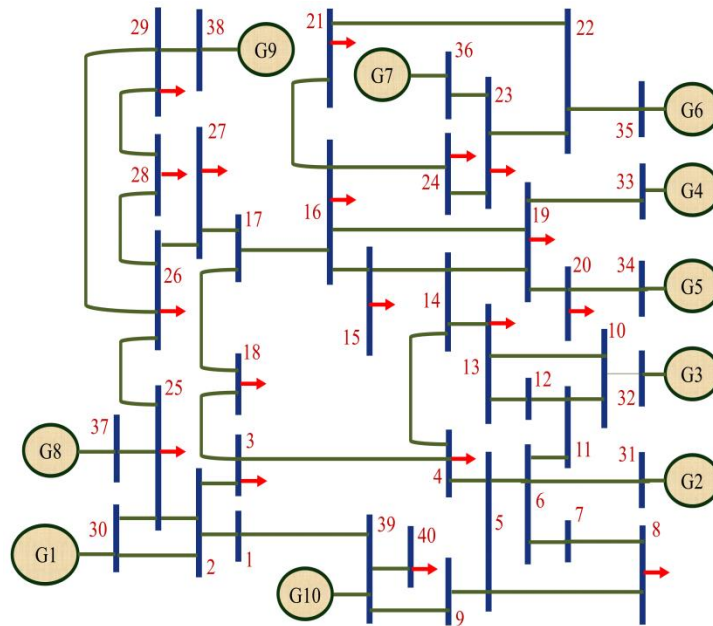


Fig. 2. Topology of modified IEEE 39-Bus system [1].

Table II. The description about modified IEEE 39-bus system [1].

Number of buses	Number of lines	Number of loads	Number of transformers	Number of generators
40	35	18	12	10

Two different scenarios are applied to the test system to evaluate the proposed load shedding scheme in this paper (M2): (1) simultaneous trips of generator 3 and transmission line (5,6), at $t=0.3s$ and (2) tripping of generator 3 at $t=0.3s$ and then tripping of generator 10 at $t=0.9s$. The subsequent tests are carried out for comparison purpose between M1 and M2. It is considerable that there are many voltage signals according to 40 buses– could be scrutinized in each scenario. Therefore, all voltage signals will be analyzed at first and after that we concentrate on the weakest load buses that are highly affected by each scenario.

A. Scenario No. 1

A-1. Test system collapse with no protective load shedding method

Voltage and frequency of the test system buses undergo a slight fluctuation, after the disturbance, as observed in Figs. (3-a) and (3-b). Controlling devices such as turbo-governors, Automatic Voltage Regulators (AVR’s) and Load Tap Changers (LTC’s) damp the fluctuations for approximately 10 seconds since the disturbance occurs. After this time, both the system frequency and voltage experience a severe oscillation owing to the disability of the controlling devices to cope with large disturbances. As a result of this fact, both frequency and voltage of the test power system collapse at $t=14.44s$. Some of the weakest load buses extremely affected by the first scenario are indicated in Fig. (3-c).

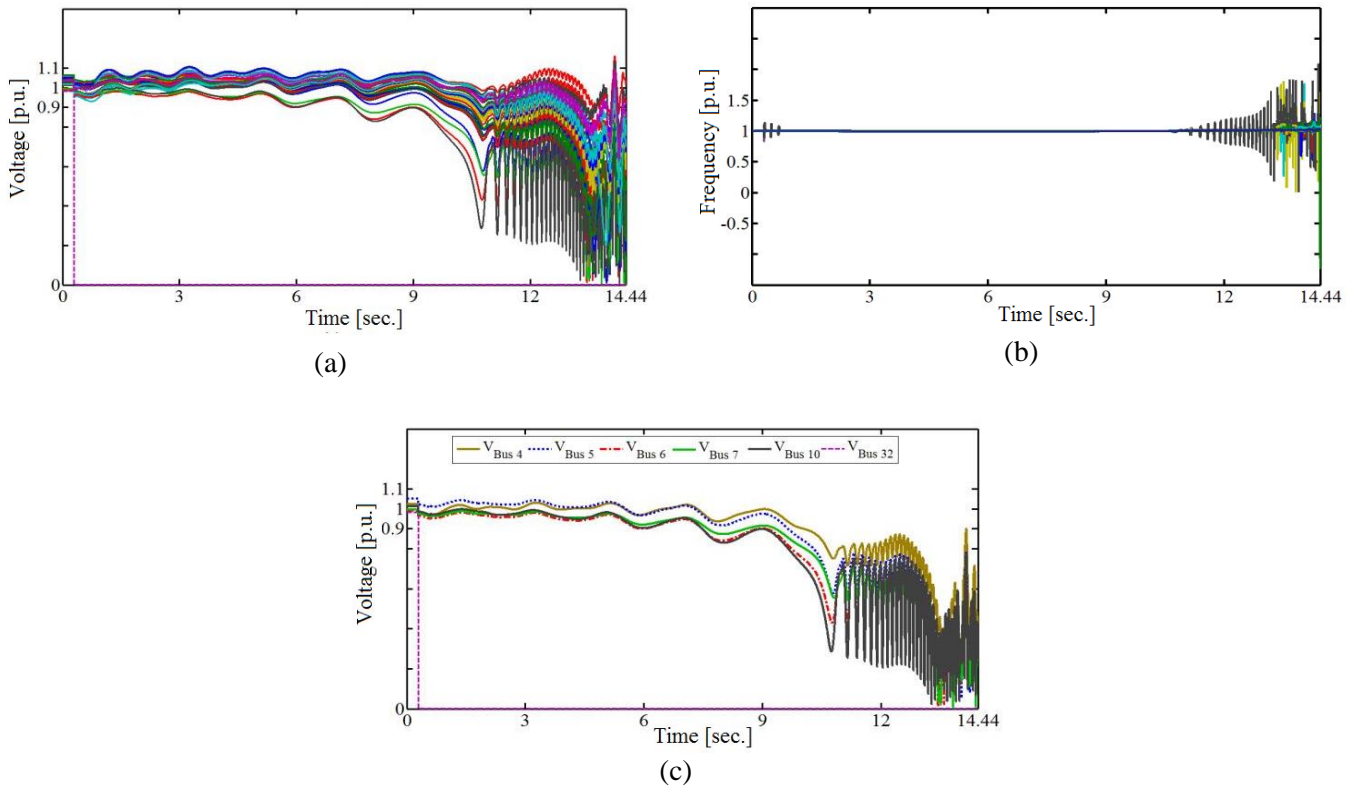


Fig. 3. Observation for the system collapse process after the first scenario without load shedding, (a) Voltage collapse of all buses, (b) Frequency collapse, (c) Extremely affected buses.

A-2. Test system stability after M1 method activation

The test power system voltage of bus 32 drops to zero point immediately and voltages of other buses experience a fluctuation approximately 0.05 pu after the disturbance as observed in Fig. (4-a). In addition, frequency of bus 32 vibrates seriously and other buses frequency undergoes a slope of 0.06 (Hz/s) as seen in Fig. (4-b). M1 method is triggered under this condition. Although, the system voltage magnitude falls down to 0.896 pu at $t=0.88s$, it stays at this value of voltage for only 0.04 seconds. As represented in Fig. (4-a), after this time, the rising trend of the voltage is commenced and it passes 0.9 pu, which it is the lowest allowable limit of voltage, at $t=0.925s$. Fig. (4-b) reports the test system frequency response after M1 scheme activation. Frequency drops seriously at $t=0.3s$; however it goes upward at $t=6s$ after employing M1 method and the fluctuation magnitude of frequency decreases gradually so that it is only 0.004 pu at $t=17.5s$. It is considerable that the frequency never passes its magnitude limits owing to M1 method. Fig. (4-c) confirms that the voltages of the critical buses come into the permissible range subsequent to applying M1 method at $t=0.925s$ and never pass this limit after this time.

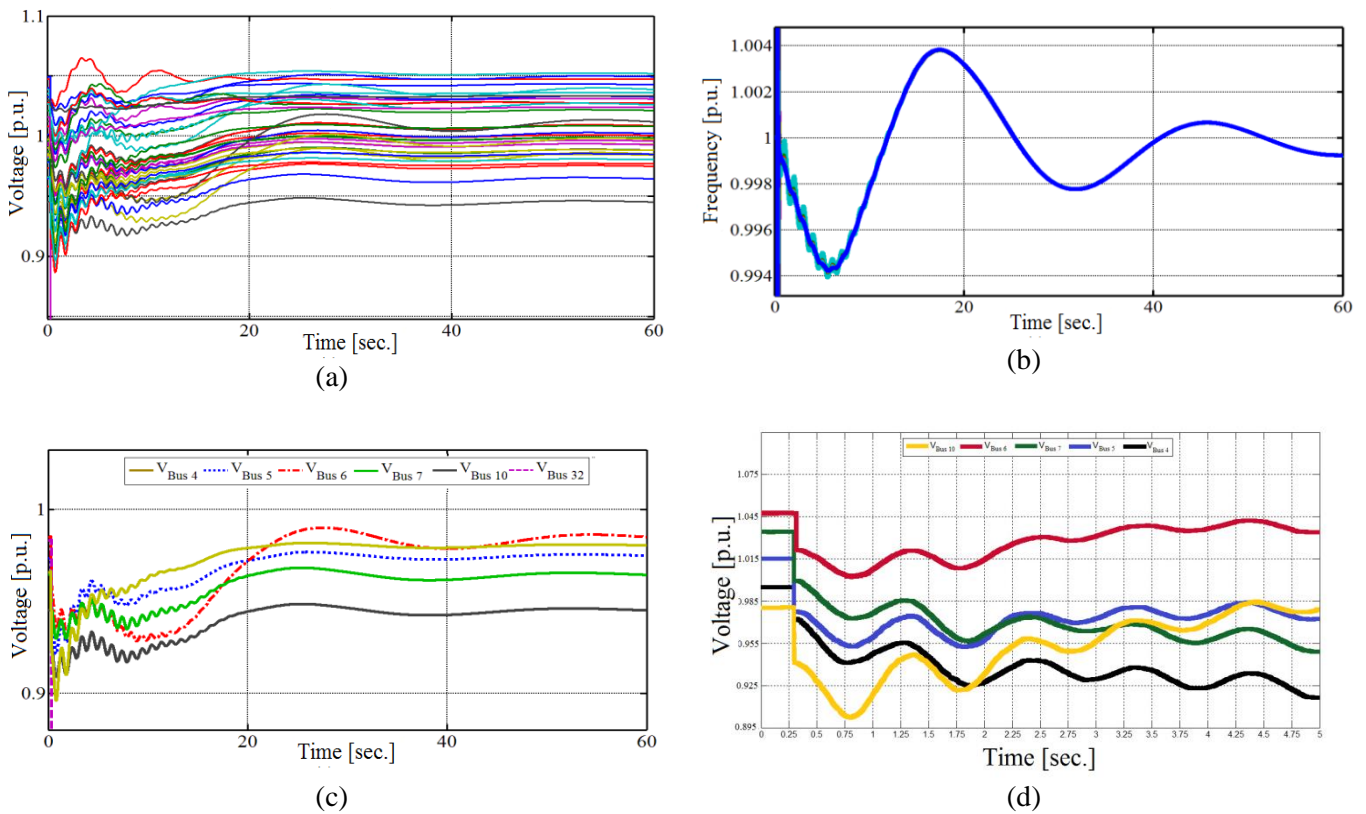


Fig. 4. System stability after the first scenario employing M1 method, (a) Voltage stability of all buses, (b) Frequency stability, (c) Voltage stability of the critical buses, (d) Details of voltage stability of the critical buses

A-3. Test system stability after M2 method activation

Both the test system voltage and frequency suffer some serious fluctuations after occurrence of the first scenario that causes M2 method be triggered. Subsequent to M2 method activation, voltage stays in 0.91 pu at $t=8.73s$ for 1.5 seconds, afterwards it has an advancement to the steady state point so that never passes its limit margin as demonstrated in Fig. (5-a). As observed in Fig. (5-b) the test system frequency experiences some vibrations after the first scenario and then it will be stable at $t=7.5s$ applying M2

method. The considerable fact about the test system frequency is that it never departs its permissible range actuating M2 method. Fig. (5-c) illustrates the voltage compartment of the critical buses after M2 method activation. It is considerable that the voltage magnitudes of the last mentioned buses settle under one per-unit after applying M1 method. While on the contrary, by means of actuating M2 method, the voltage magnitudes of the critical load buses come into contact with levels greater than one per-unit several times. This is a good reason why M2 method has a better performance when it confronts the first scenario. Fig. (6-a) depicts the employed total Pareto Fronts in order to select the weakest load buses to start load shedding from, while Fig. (6-b) represents the set of Pareto Fronts for shedding of active and reactive powers, after M2 method activation following the first scenario.

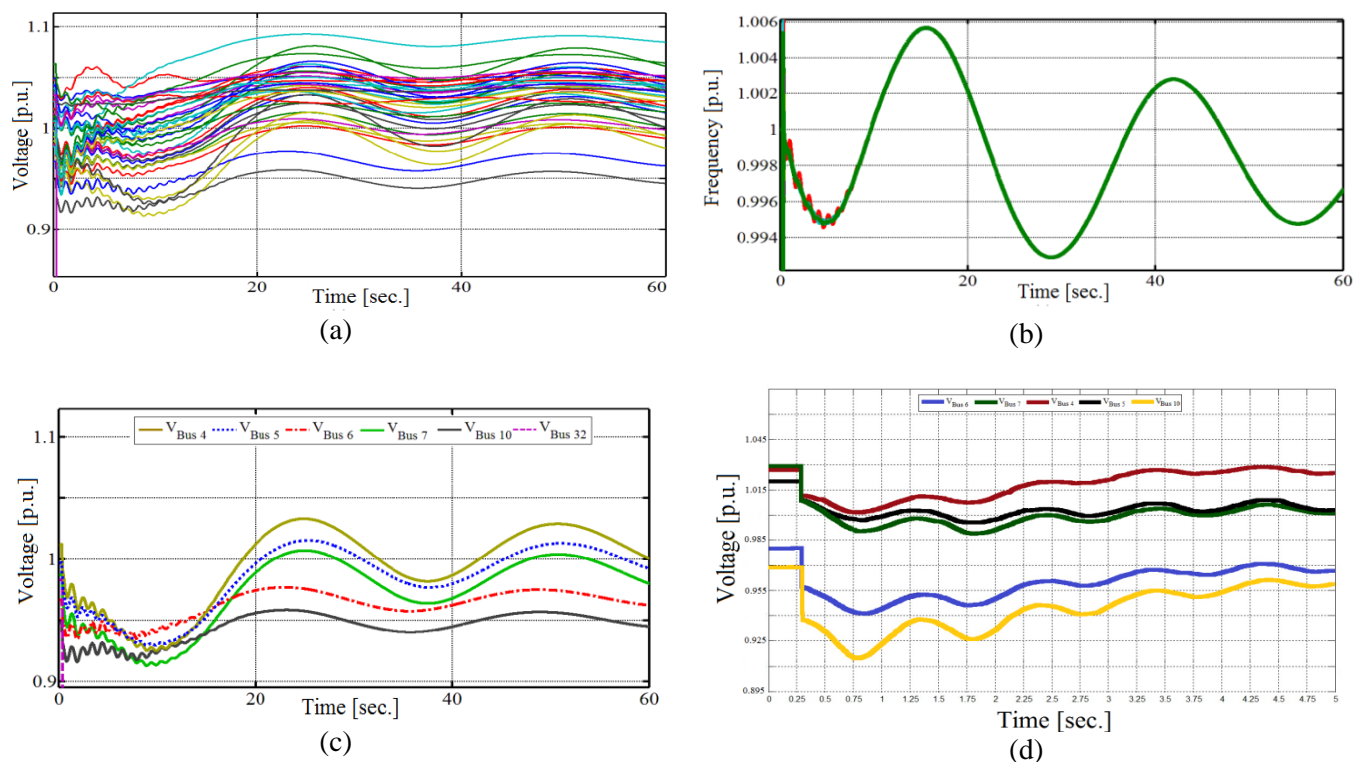


Fig. 5. System stability after the first scenario employing M2 method, (a) Voltage stability of all buses, (b) Frequency stability, (c) Voltage stability of the critical buses, (d) Details of voltage stability of the critical buses

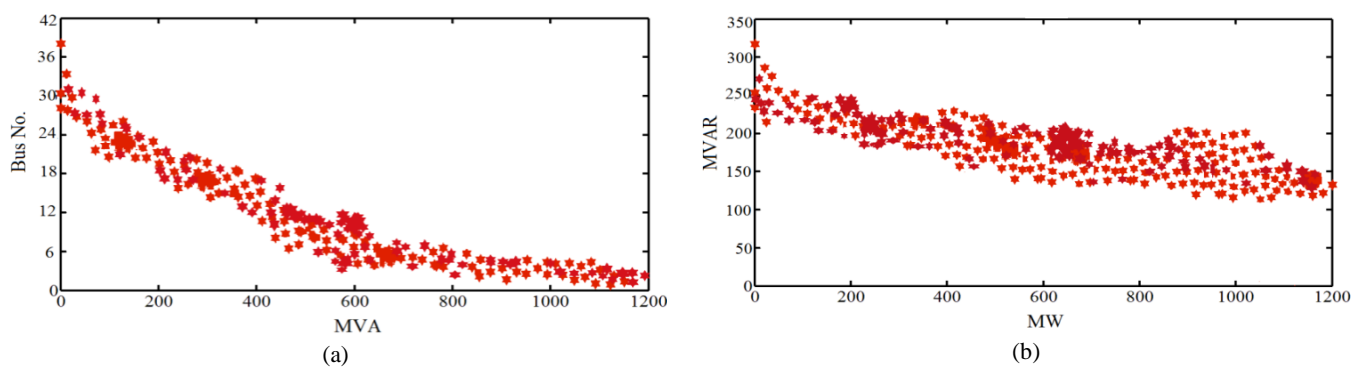


Fig. 6. The total Pareto Fronts after the first scenario utilizing M2 method, (a) Selecting of the weakest load buses to commence load shedding, (b) Estimation of active and reactive powers to be shed from the selected load buses.

B. Scenario No. 2

B-1. Test system collapse with no protective load shedding method

The voltage of the test system drops approximately 0.15 pu subsequent to the trip of G3 at $t=0.3s$; consequently, controlling devices are activated to compensate this fall in a short time. As represented in Fig. (7-a), after G10 outage, the test system experiences another voltage drop one more time. The Controlling devices prevent the test power system from collapsing for only 0.3 seconds after G10 outage that results in the second voltage drop at $t=1.2s$, and eventually the total voltage collapse occurs at $t=3.43s$. The test system frequency deviates after both G3 and G10 trips as observed in Fig. (7-b). Frequency fluctuation magnitude is restricted in the preset range utilizing controlling devices at $t=1s$. Although, the persisting disturbance leads to increasing fluctuation magnitude at $t=2.2s$ once more and ultimately, the test system frequency collapses at $t=3.43s$. Considering the test system collapse condition after the second scenario, it is a demanding challenge that M1 and M2 methods will have to confront with. Voltages of some most affected buses are shown in Fig. (7-c).

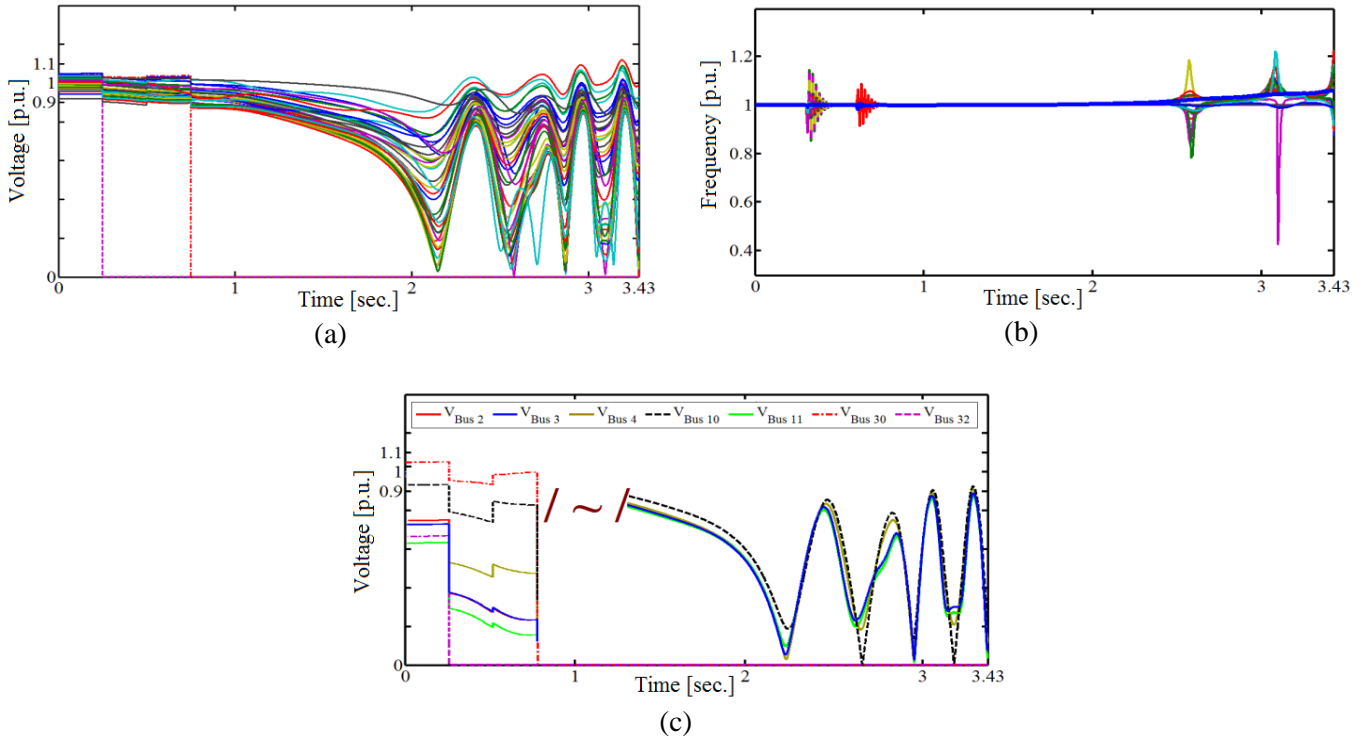


Fig. 7. System collapse after the second scenario without load shedding, (a) Voltage collapse of all buses, (b) Frequency collapse, (c) Extremely affected buses.

B-2. Test system stability after M1 method activation

M1 method is activated after G3 outage, and commences to shed loads according to Table I to achieve the power system stability once more. The first load shedding stage of M1 method prevents the voltage magnitude reduction after 0.3 seconds. G10 trip causes the voltage magnitude to decrease one more time at $t=0.9s$ that triggers the second stage of load shedding of M1 method. M1 method is not capable of stabilizing the test system in the first stage of load shedding, due to the short interval between G3 and G10 trips. For this reason the further voltage fluctuation starts at $t=6s$. As considered in Fig. (8-a), the voltage magnitude meets 0.816 pu at $t=10.9s$ despite M1 activation. Notwithstanding M1 method struggle to increase voltage magnitude at about 11 seconds after G10 outage by means of progressive

load shedding, it requires approximately 20 seconds to augment bus voltages up to 0.9 pu. The test system frequency comportment is not much satisfactory after the first load shedding phase of M1 method. G10 outage intensifies the frequency fluctuations one more time. Seen from Fig. (8-b) these disturbances have acute influences on the test frequency stability that prohibits it from approaching the permissible limit until $t=23.3$ s, despite the fact that M1 method is activated currently. Voltages comportment of the critical buses introduced in Fig. (7-c) is analyzed in Fig. (8-c) after M1 method activation under the second scenario.

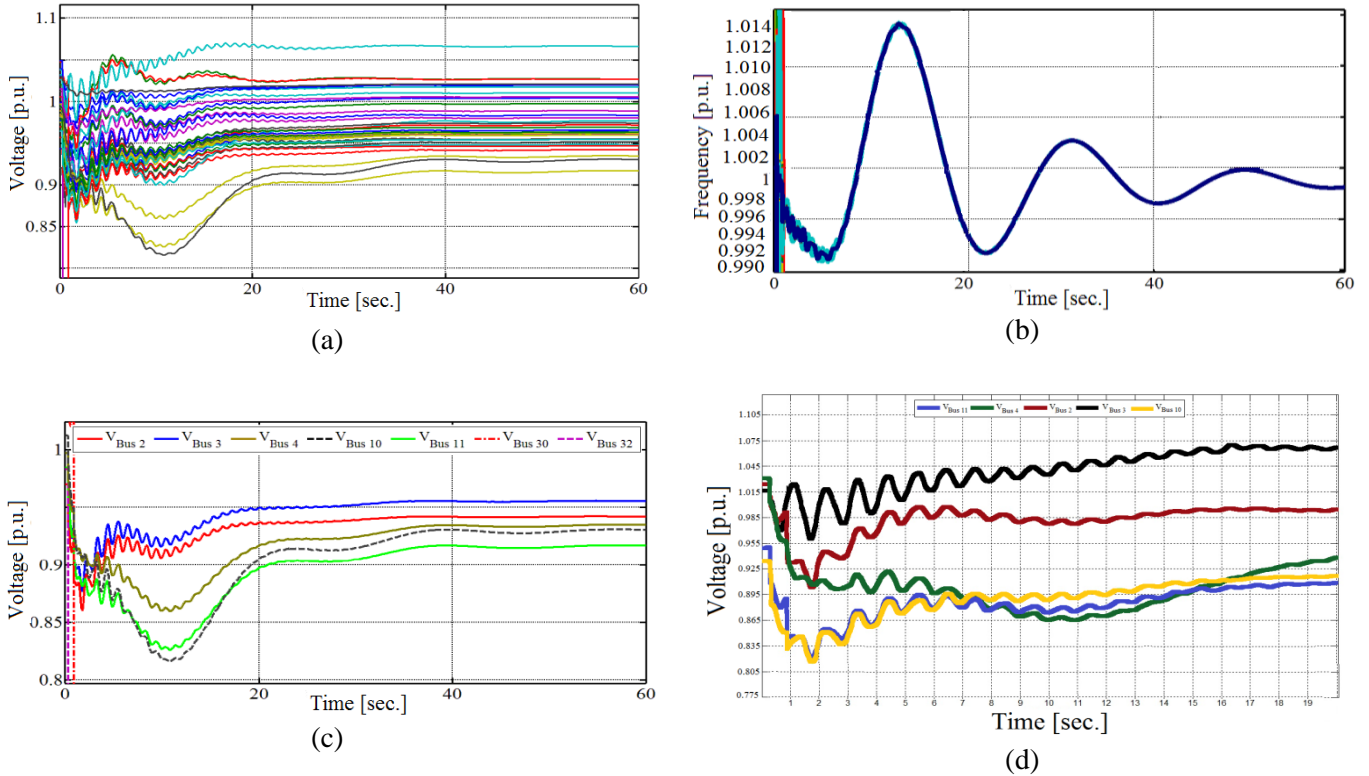


Fig. 8. System stability after the second scenario employing M1 method, (a) Voltage stability of all buses (b) Frequency stability, (c) Voltage stability of the critical buses, (d) Details of voltage stability of the critical buses

B-3. Test system stability after M2 method activation

The test system voltage magnitude decreases approximately 0.15 pu subsequent to G3 outage. Controlling devices make an abortive attempt to satisfy this decrement in voltage magnitude. Considering this amount of voltage drop does not trigger M2 method of load shedding, the voltage magnitude still declines due to the mechanical constraints of controlling devices insomuch that the voltage passes downwards 0.9 pu at $t=0.65$ s as represented in Fig. (9-a). At this time, M2 method is triggered and commences to raise the voltage magnitude. The test system voltage declines following G10 outage at $t=0.9$ s once more and results in the trigger of the second stage of M2 method. Owing to the short interval between G3 outage and G10 outage, the first estimation of load shedding made by M2 method is not so accurate. Therefore, there is a further voltage drop at $t=1.2$ s. In other words, trigger of the second stage of M2 method is based upon the first steady state information of the test system; and while the first stage of load shedding is taking place. Consequently, the second stage of load shedding is started in a transient situation. This causes an inaccurate estimation in the second stage of load shedding of M2 method. Hence the weakest load buses to start load shedding from and/or the amount of active or reactive power to be shed from the predefined load buses are not selected exactly. Seen from

Figs. (9-a) and (9-c), the second load shedding estimation of M2 method requires approximately 5 seconds in order to effectuate a slight increment in the voltage magnitude. Since there is a time interface between the first and the second stages of M2 method load shedding, the test system experience a voltage drop at $t=7s$ once more. This results in a third stage of load shedding. The third stage of load shedding constrains the voltage drop after 4 seconds. Therefore, M2 method directs the system voltage to the predefined permissible limit after a three-stage load shedding at $t=15.6 s$. According to the changes of the test system frequency indicated in Fig. (9-b) it could be found out the frequency is restricted to its stability range after the disturbance owing to M2 method. Thus the test system frequency is never affected by a serious oscillation. M2 method approach to control the voltage limit for the critical buses mentioned in Fig. (7-c) under the second scenario is observed in Fig. (9-c). Fig. (9-e) indicates the total Pareto Fronts employed to designate the weakest load buses as the load shedding should be started at, while Fig. (9-f) represents the set of Pareto Fronts for shedding of active and reactive powers from the selected load buses, after M2 activation following the second scenario. A summary of the test results is presented in Table III to compare the approaches of M1 and M2 methods to the mentioned scenarios.

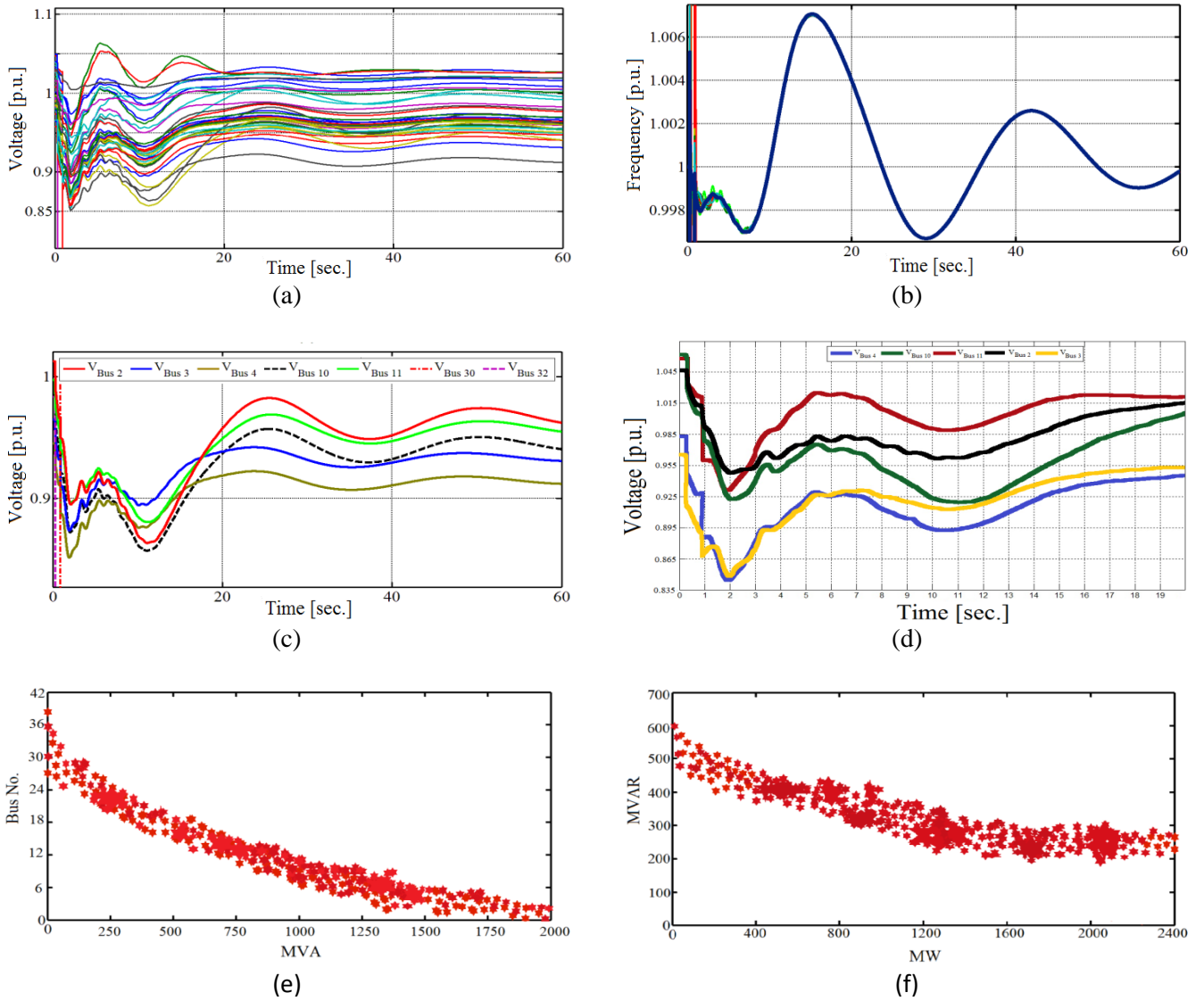


Fig. 9. System stability after the second scenario employing M2 method and the total Pareto fronts after the second scenario utilizing M2 method, (a) Voltage stability of all buses, (b) Frequency stability, (c) Voltage stability of the critical buses, (d) Details of voltage stability of the critical buses, (e) Selecting of the weakest load buses to start load shedding, (f) Estimation of active and reactive powers to be shed from the selected load buses.

Table III. Summary of system stability results after two scenarios employing m1 and m2 methods.

Measured parameter	Scenario No. 1		Scenario No. 2	
	M1 method	M2 method	M1 method	M2 method
Active power after L.S. (MW)	6222.85	6246.65	5043.87	5104.67
Reactive power after L.S. (MVar)	1308.08	1344.65	1048.89	1146.05
First stability time of voltage (s)	0.925	0.3	21	15.6
First stability time of frequency (s)	0.3	0.33	23.3	0.971
Min. voltage magnitude (pu)	0.896	0.913	0.816	0.852
Max. voltage magnitude (pu)	1.063	1.093	1.070	1.063
Min. frequency magnitude (pu)	0.9938	0.9932	0.9907	0.9967
Max. frequency magnitude (pu)	1.0039	1.0056	1.0143	1.0071

7. CONCLUSION

To overcome the disadvantages of the existing combinational load shedding methods, a load shedding scheme based on a new load shedding distribution method, using combined frequency and voltage stability assessment, is employed in this work. The GA is utilized throughout the proposed load shedding process to select the most critical load buses. Thus the number of participating load buses in the total power imbalance distribution decreases considerably. As an innovation of this paper, reactive power is employed directly into the reactive power load shedding distribution together with active power load shedding distribution, to address the voltage stability issue immediately and more efficiently in the load shedding process. The test results confirm the capability of M2 method rather than M1 method coming across difficult scenarios. They also corroborate that the improvements in load shedding distribution technique can enhance the steady state of power systems in terms of both frequency and voltage stability with a good transient comportment, when a power system encounters acute disturbances. Thus, there is a novel alternative to protect the system safely and efficiently for the load shedding in practical applications.

REFERENCES

- [1] I. Kaffashan, T. Amraee, "Probabilistic undervoltage load shedding using point estimate method", *IET Generation, Transmission and Distribution*, Vol. 9, No. 15, pp. 2234-2244, Nov. 2015.
- [2] A.C. Adewole, R. Tzoneva, A. Apostolov, "Adaptive under-voltage load shedding scheme for large interconnected smart grids based on wide area synchrophasor measurements", *IET Generation, Transmission and Distribution*, Vol. 10, No. 8, pp. 1957-1968, May 2016.
- [3] G. Shahgholian, M. Ebrahimi-Salary, "Effect of load shedding strategy on interconnected power systems stability when a blackout occurs", *International Journal of Computer and Electrical Engineering*, Vol. 4, No. 2, pp. 212-216, April 2012.
- [4] A. Mahari, H. Seyedi, "A wide area synchrophasor-based load shedding scheme to prevent voltage collapse", *International Journal of Electrical Power and Energy Systems*, Vol. 78, pp. 248-257, June 2016.
- [5] A. Estebarsari, E. Pons, T. Huang, E. Bompard, "Techno-economic impacts of automatic under voltage load shedding under emergency", *Electric Power Systems Research*, Vol. 131, pp. 168-177, Feb. 2016.
- [6] A. Ahmadi, Y. Alinejad-Beromi, "A new integer-value modeling of optimal load shedding to prevent voltage instability", *International Journal of Electrical Power and Energy Systems*, Vol. 65, pp. 210-219, Feb. 2015.

- [7] U. Rudez, R. Mihalic, "Analysis of under frequency load shedding using a frequency gradient", *IEEE Trans. on Power Delivery*, Vol. 26, No. 2, pp. 565-575, April 2011.
- [8] Y.Y. Hong, P. H. Chen, "Genetic-based under-frequency load shedding in a stand-alone power system considering fuzzy loads", *IEEE Trans. on Power Delivery*, Vol. 27, N0. 1, pp. 87-95, Jan. 2012.
- [9] Y.Y. Hong, S. F. Wei, "Multi-objective under-frequency load shedding in an autonomous system using hierarchical genetic algorithms", *IEEE Trans. on Power Delivery*, Vol. 25, No. 3, pp. 1355-1362, July 2010.
- [10] H. Alkhatib, J. Duveau, "Dynamic genetic algorithms for robust design of multimachine power system stabilizers", *International Journal of Electrical Power and Energy Systems*, Vol. 45, pp. 242–251, 2013.
- [11] W.P. Luan, M.R. Irving, J.S. Daniel, "Genetic algorithm for supply restoration and optimal load shedding in power system distribution networks", *IET Generation, Transmission and Distribution*, Vol. 149, No. 2, pp. 145-151, March 2002.
- [12] M. Haomin, K. Wing Chan, L. Mingbo, "An intelligent control scheme to support voltage of smart power systems", *IEEE Trans. on Power Industrial Informatics*, Vol. 9, No. 3, pp. 1404–1414, Aug. 2013.
- [13] F. Daneshfar, H. Bevrani, "Load-frequency control: a GA-based multi-agent reinforcement learning", *IET Generation, Transmission and Distribution*, Vol. 4, No. 1, pp.13-26, 2010.
- [14] A. Saffarian, M. Sanaye-Pasand, "Enhancement of power system stability using adaptive combination-al load shedding methods", *IEEE Trans. on Power Systems*, Vol. 26, No. 3, pp. 1010-1020, Aug 2011.
- [15] A.P. Ghaleh, M. Sanaye-Pasand, A. Saffarian, "Power system stability enhancement using a new combinational load shedding algorithm", *IET Generation, Transmission and Distribution*, Vol. 5, No. 5, pp. 551-560, May 2011.
- [16] J. Tang, J. Liu, F. Ponci, A. Monti, "Adaptive load shedding based on combined frequency and voltage stability assessment using synchrophasor measurements", *IEEE Trans. on Power Systems*, Vol. 28, No. 2, pp. 2035-2047, May 2013.
- [17] P.M. Joshi, "Load shedding algorithm using voltage and frequency data", Clemson University, Dec. 2007.
- [18] W. Qin, P. Wang, X. Han, X. Du, "Reactive power aspects in reliability assessment of power systems", *IEEE Trans. on Power Systems*, Vol. 26, No. 1, pp. 85-92, Feb. 2011.
- [19] R. Zarate, "Optimal power flow with stability constrains", PhD Thesis at Department of Electrical Engineering, Ciudad Real, July 2010.
- [20] P.M. Anderson, M. Mirheydar, "A low-order system frequency response model", *IEEE Trans. on Power Systems*, Vol. 5, No. 3, pp. 720-729, August 1990.
- [21] D.L.H. Aik, "A general-order system frequency response model incorporating load shedding: analytic modeling and applications", *IEEE Trans. on Power Systems*, Vol. 21, No. 2, pp. 709-717, May 2006.
- [22] IEE Std., "IEEE guide for the application of protective relays used for abnormal frequency load shedding and restoration", IEE Std., C37.117-2007, Aug. 2007.